Direct amplitude shaping of high harmonics in the extreme ultraviolet

D. Kiselev,[1] P. M. Kraus,[2] L. Bonacina,[1] H.J. Wörner,[2,3] and J.P. Wolf[1,*]

[1]*GAP, University of Geneva, 1205 Geneva, Switzerland*
[2]*Physikalische Chemie, ETH Zürich, 8093 Zürich, Switzerland*
[3]*woerner@phys.chem.ethz.ch*
[*]*jean-pierre.wolf@unige.ch*

Abstract: We demonstrate direct amplitude shaping of high harmonics (HHs) using a reflective micromirror array based on micro-electro-mechanical-system (MEMS) technology. We show independent control over the intensity of each HH in the observed range (14 – 36 eV). These results are used to calculate the control achieved over the temporal structure of the attosecond pulses in the train.

OCIS codes: (320.5540) Pulse shaping; (190.2620) Harmonic generation and mixing.

References and links

1. A. M. Weiner, "Femtosecond pulse shaping using spatial light modulators," Rev. Sci. Instrum. **71**, 1929–1960 (2000).
2. C. C. Chang, H. P. Sardesai, and A. M. Weiner, "Dispersion-free fiber transmission for femtosecond pulses by use of a dispersion-compensating fiber and a programmable pulse shaper," Opt. Lett. **23**, 283–285 (1998).
3. H. X. Miao, A. M. Weiner, L. Mirkin, and P. J. Miller, "Wideband deterministic all-order polarization-mode dispersion generation via pulse shaping," IEEE Photon. Technol. Lett. **20**, 159–161 (2008).
4. B. W. Xu, J. M. Gunn, J. M. Dela Cruz, V. V. Lozovoy, and M. Dantus, "Quantitative investigation of the multiphoton intrapulse interference phase scan method for simultaneous phase measurement and compensation of femtosecond laser pulses," J. Opt. Soc. Am. B **23**, 750–759 (2006).
5. J. D. McKinney, I. S. Lin, and A. M. Weiner, "Shaping the power spectrum of ultra-wideband radio-frequency signals," IEEE Trans. Microw Theory Tech. **54**, 4247–4255 (2006).
6. M. Aeschlimann, M. Bauer, D. Bayer, T. Brixner, F. J. de Abajo, W. Pfeiffer, M. Rohmer, C. Spindler, and F. Steeb, "Adaptive subwavelength control of nano-optical fields," Nature **446**, 301–304 (2007).
7. N. Dudovich, D. Oron, and Y. Silberberg, "Single-pulse coherently controlled nonlinear Raman spectroscopy and microscopy," Nature **418**, 512–514 (2002).
8. J. L. Herek, W. Wohlleben, R. J. Cogdell, D. Zeidler, and M. Motzkus, "Quantum control of energy flow in light harvesting," Nature **417**, 533–535 (2002).
9. M. Roth, L. Guyon, J. Roslund, V. Boutou, F. Courvoisier, J. P. Wolf, and H. Rabitz, "Quantum control of tightly competitive product channels," Phys. Rev. Lett. **102**, 253001 (2009).
10. R. Lopez-Martens, K. Varju, P. Johnsson, J. Mauritsson, Y. Mairesse, P. Salieres, M. B. Gaarde, K. J. Schafer, A. Persson, S. Svanberg, C. G. Wahlstrom, and A. L'Huillier, "Amplitude and phase control of attosecond light pulses," Phys. Rev. Lett. **94**, 033001 (2005).
11. R. Bartels, S. Backus, E. Zeek, L. Misoguti, G. Vdovin, I. P. Christov, M. M. Murnane, and H. C. Kapteyn, "Shaped-pulse optimization of coherent emission of high-harmonic soft X-rays," Nature **406**, 164–166 (2000).
12. D. M. Healion, I. V. Schweigert, and S. Mukamel, "Probing multiple core-hole interactions in the Nitrogen K-edge of DNA base pairs by multidimensional attosecond X-ray spectroscopy. A simulation study," J. Phys. Chem. A **112**, 11449–11461 (2008).
13. A. Willner, F. Tavella, M. Yeung, T. Dzelzainis, C. Kamperidis, M. Bakarezos, D. Adams, M. Schulz, R. Riedel, M. C. Hoffmann, W. Hu, J. Rossbach, M. Drescher, N. A. Papadogiannis, M. Tatarakis, B. Dromey, and M. Zepf, "Coherent control of high harmonic generation via dual-gas multijet arrays," Phys. Rev. Lett. **107**, 175002 (2011).
14. D. H. Reitze, S. Kazamias, F. Weihe, G. Mullot, D. Douillet, F. Auge, O. Albert, V. Ramanathan, J. P. Chambaret, D. Hulin, and P. Balcou, "Enhancement of high-order harmonic generation at tuned wavelengths through adaptive control," Opt. Lett. **29**, 86–88 (2004).

#174409 - $15.00 USD Received 16 Aug 2012; revised 18 Sep 2012; accepted 18 Sep 2012; published 1 Nov 2012

15. T. Pfeifer, D. Walter, C. Winterfeldt, C. Spielmann, and G. Gerber, "Controlling the spectral shape of coherent soft X-rays," Appl. Phys. B. Lasers Opt. **80**, 277–280 (2005).
16. S. M. Weber, L. Bonacina, W. Noell, D. Kiselev, J. Extermann, F. Jutzi, S. Lani, O. Nenadl, J. P. Wolf, and N. F. de Rooij, "Design, simulation, fabrication, packaging, and characterization of a MEMS-based mirror array for femtosecond pulse-shaping in phase and amplitude," Rev. Sci. Instrum. **82**, 075106 (2011).
17. J. T. Zhu, S. K. Zhou, H. C. Li, Q. S. Huang, Z. S. Wang, K. Le Guen, M. H. Hu, J. M. Andre, and P. Jonnard, "Comparison of Mg-based multilayers for solar He II radiation at 30.4 nm wavelength," Appl Optics **49**, 3922–3925 (2010).
18. A. Rupenyan, J. B. Bertrand, D. M. Villeneuve, and H. J. Worner, "All-optical measurement of high-harmonic amplitudes and phases in aligned molecules," Phys. Rev. Lett. **108**, 033903 (2012).
19. J. Extermann, S. M. Weber, D. Kiselev, L. Bonacina, S. Lani, F. Jutzi, W. Noell, N. F. de Rooij, and J. P. Wolf, "Spectral phase, amplitude, and spatial modulation from ultraviolet to infrared with a reflective mems pulse shaper," Opt. Express **19**, 7580–7586 (2011).
20. F. Frassetto, C. Cacho, C. A. Froud, I. C. E. Turcu, P. Villoresi, W. A. Bryan, E. Springate, and L. Poletto, "Single-grating monochromator for extreme-ultraviolet ultrashort pulses," Opt. Express **19**, 19169–19181 (2011).
21. L. Poletto, P. Villoresi, E. Benedetti, F. Ferrari, S. Stagira, G. Sansone, and M. Nisoli, "Intense femtosecond extreme ultraviolet pulses by using a time-delay-compensated monochromator," Opt. Lett. **32**, 2897–2899 (2007).
22. Y. Mairesse, A. de Bohan, L. J. Frasinski, H. Merdji, L. C. Dinu, P. Monchicourt, P. Breger, M. Kovacev, R. Taieb, B. Carre, H. G. Muller, P. Agostini, and P. Salieres, "Attosecond synchronization of high-harmonic soft X-rays," Science **302**, 1540–1543 (2003).

1. Introduction

Pulse shaping of ultrashort laser pulses by phase and amplitude manipulation of their spectral components in Fourier space [1] has proved a very effective tool in a variety of photonics and spectroscopy applications, ranging from fiber communications [2, 3], waveform characterization [4], radio frequency photonics [5] to nonlinear microscopy [6, 7] and coherent quantum control [2, 8, 9]. Although these works addressed very diverse spectral regions, to date a complete and independent control over the spectral amplitude and phase of HHs has been hindered by the technological difficulties associated with XUV optics. Reported attempts related to the use of thin aluminium filters introduced in the HH beam path, for obtaining compressed attosecond pulses [10]. Alternatively, some authors have acted upon the driving laser pulses to manipulate HH generation [11–15]. In this context, Reitze *et al*. and Pfeifer *et al*. have modified via an adaptive loop approach the spectral phase of the driving field obtaining enhanced HH generation efficiency and arbitrarily shaped spectra in the soft X-ray region.

The approach we present here is based on a MEMS reflective device that we have recently developed [16]. The latter, which has already proven successful for pulse-shaping of deep UV pulses [16], has been adapted to amplitude shaping of HHs in the XUV. We show independent control over the intensity of each high harmonic in the $14-36$ eV range, which leads to the control over the temporal structure of the attosecond pulses in the train as we show through explicit calculations in the last section.

2. Experimental

Figure 1 shows the experimental setup. The 100 micromirrors MEMS device has been described in reference [16]. Its unique stroke (up to 3 μm) and tilt (up to 1.2°) capabilities allow simultaneous amplitude and phase shaping, when placed in the Fourier plane of a folded zero-dispersion *4f* arrangement. Each mirror measures 160x1000 μm^2, with 3 μm gap between adjacent mirrors, yielding a high fill factor $> 98\%$. A very important aspect for XUV applications is surface flatness and minimal deformation. The device is designed (thick 35 μm mirrors and X-shaped springs) such that deformation and stress are minimized. The surface roughness, taking into account the presence of Ti/Al coating, amounts to less than 16 nm peak to valley (PTV). Together with the very small gaps between the mirrors, our design leads to no observable perturbations of the spatial intensity profile after reflection as compared to the incident XUV beam.

#174409 - $15.00 USD Received 16 Aug 2012; revised 18 Sep 2012; accepted 18 Sep 2012; published 1 Nov 2012

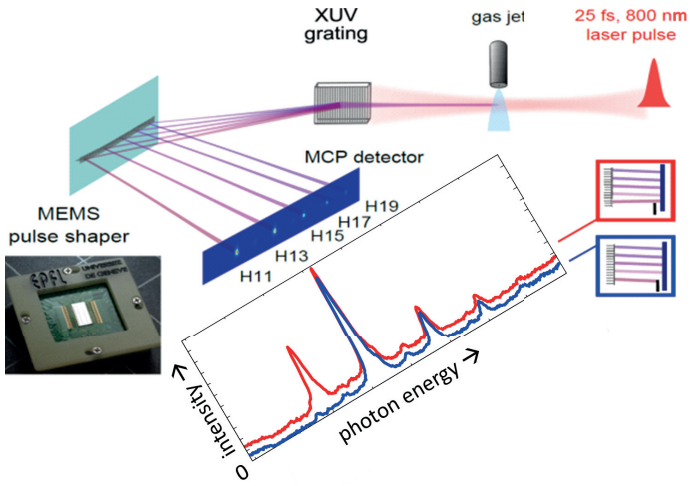

Fig. 1. High-harmonic pulse shaping experiment in the XUV: The HHs generated in the gas jet are spectrally dispersed and focused onto a MCP detector via a reflective linear micromirror array (MEMS), which can individually control the reflection angle of each HH separately and deviate it onto a spatial filter (mask), as shown in the insets in red and blue rectangles. The red line shows the unshaped spectrum (shifted vertically for clarity) and the blue line shows the spectrum with maximal attenuation of H11.

The second critical aspect for XUV applications is clearly the choice of a suitable reflective coating. In the present experiment, we found that a 10/300 nm Ti/Al metal coating provides an acceptable compromise between reflectivity, adhesion, and stress in the mirrors. At our incidence angle (20-25°) and spectral range, the aluminum coating reflectivity is of the order of a percent, which is sufficient for many further experiments. For improving the reflectivity at higher energies, special multi-layer coatings will have to be applied, such as Mg/SiC [17].

HH radiation is generated by focusing (f = 40 mm) a fraction (0.7 mJ) of the output of an amplified titanium-sapphire femtosecond laser system (Coherent, 800 nm, 8 mJ, 1 kHz, 25 fs) into a pulsed supersonic expansion of argon or ethylene in a high vacuum chamber [18]. An Even-Lavie nozzle with a repetition rate of 1 kHz is used to generate a dense, well-collimated gas jet. HH radiation further propagates into an extreme-ultraviolet spectrometer consisting of a 120 μm wide entrance slit and an aberration-corrected concave holographic grating with 1200 lines/mm (Shimadzu 30-002). The grating disperses the high-harmonic radiation in the horizontal plane while allowing it to freely diverge in the vertical direction. The far-field spectrally-dispersed high-harmonic profile is recorded either directly in the focal plane of the concave grating with a microchannel-plate detector backed with a phosphor screen or following reflection on the MEMS device. In both cases, the spectrally-dispersed high-harmonic profiles are recorded using a charge-coupled device camera.

3. Results and discussions

The spectral range that we successfully addressed encompasses the region from H9 (14 eV) to H23 (36 eV). We observed a significant decrease of the HHs intensity above 40 eV, due to the reflectivity of the aluminium MEMS coating, and its possible oxidation by contamination. The beam quality of the reflected HHs by the MEMS device is excellent, with no observable

#174409 - $15.00 USD Received 16 Aug 2012; revised 18 Sep 2012; accepted 18 Sep 2012; published 1 Nov 2012

diffraction due to pixellisation or degraded profile due to insufficient surface flatness (16 nm peak to valley).

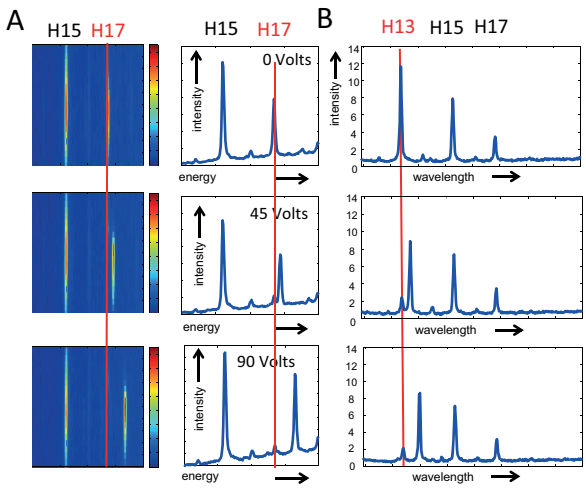

Fig. 2. Selective displacement of HHs. (A) Displacement of H17 as a function of the applied voltage, observed on the MCP and vertically averaged energy plots. (B) HH-selective variable beamsplitter: 4/5 of the intensity of H13 is displaced while 1/5 remains at the same location (i.e. it conserves the same ***k***-vector).

Figure 2(A) displays a typical example of a selective displacement of one HH (H17, 26 eV), leaving the other harmonics unaffected. The six mirrors illuminated by H17 are tilted progressively from 0° to 1.2° by changing the applied voltage. In the on-line supplementary material, a movie (Media 1) is available, displaying the continuous displacement of H15 on the MCP, while H13, 17 and 19 remain at their original position. Obviously, if only some of the illuminated micromirrors are tilted, a HH- selective variable beamsplitter is created, with a branching ratio and an angle that can be adjusted by the number and the amplitude of the tilted mirrors (Fig. 2(B)).

In order to achieve amplitude shaping, a mask that blocks the tilted fraction of the HH intensity was installed. The gray-scale amplitude modulation of the HHs is then achieved by tilting between 0 and 12 of the illuminated mirrors (for H11) as displayed in Fig. 3. A movie is available online showing the modulation of H11 (slow, Media 2) and H15 (fast, Media 3). In this experiment, the mask consisted of a single slit, located at the position of the lowest HH in the observed spectrum. For changing the detected spectral range, the concave XUV grating was accordingly moved (using a motorized mount). The same amplitude control was also applied to other individual HHs (see supplementary movies Media 2 and Media 3), or to an arbitrary sub-set of them. Straightforward HH amplitude functions are, for instance, filtering out a single harmonic, low-pass, high-pass or band-pass filtering, constant amplitude for all HHs over a defined spectral domain, etc. but any function should ultimately be possible to realize, within the limits allowed by the number of illuminated pixels per HH. Obviously, more sophisticated masks with multiple slits, adapted to the whole set of HHs, can be constructed and adapted to the purpose of future experiments. Very interestingly, tilt motion can be used not only for amplitude modulation but also for achieving ***k*** vector optimization [19] in multi-XUV wave mixing experiments such as those theoretically proposed by S. Mukamel [12].

In a *4f*-type zero-dispersion arrangement (i.e. an arrangement where the modulated HHs are

#174409 - $15.00 USD Received 16 Aug 2012; revised 18 Sep 2012; accepted 18 Sep 2012; published 1 Nov 2012

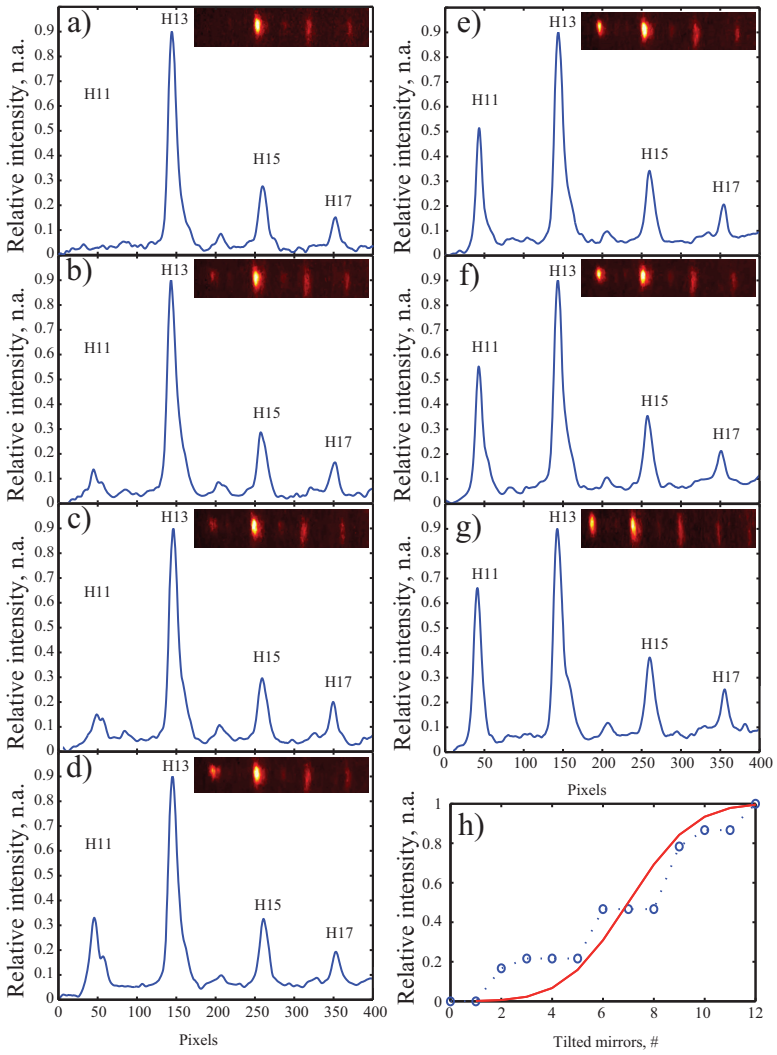

Fig. 3. Gray-scale amplitude shaping of H11 from 0 to 100%, obtained by progressively tilting 0-12 of the illuminated micromirrors as observed on the MCP (a-g). (h) HH intensity as function of the activated mirrors. The step-like behavior is caused by the limited number of working mirrors on the MEMS chip [16].

spatially recombined upon reflection back onto the XUV grating), a mask would not be necessary as tilted HHs would be geometrically displaced by several mm at the target position, and thus easily blocked before reaching it (for a quantitative dimensioning of such arrangements, see reference [13]). The overall throughput of such a device can be explicitly calculated from the specifications of commercially available components [20] to be around 0.5%. This value accounts for a gold coated device at 0° incidence, and can be further increased by applying a Mg/SiC coating [17].

In the following, we evaluate the effect of the achieved pulse shaping on the temporal shape of the attosecond pulse train corresponding to the observed HH spectrum. In this work, we did not carry out the experimental characterization of the temporal profile of the pulses, which

#174409 - $15.00 USD Received 16 Aug 2012; revised 18 Sep 2012; accepted 18 Sep 2012; published 1 Nov 2012

needs a dedicated setup like the one described by Poletto *et al*. [21]. We represent the total electric field E_{XUV} by summing up the contributions of the observed HHs with their respective measured intensities

$$E_{XUV}(t) = \sum_{q=11}^{19} A_q exp[-i\omega_q t + i\varphi(\omega_q)]$$

where q represents the harmonic order, $A_q = \sqrt{I_q}$ the amplitude of harmonic q calculated from its experimental intensity, I_q, ω_q the frequency, and, finally, $\varphi(\omega_q)$ the spectral phase. In this work, we realized amplitude shaping by modifying the A_q in a controlled way. The spectral phases $\varphi(\omega_q)$ can also be controlled by the present MEMS device, which provides both tilt and stroke capabilities [19], but a full spectral and temporal characterization would require a dedicated experimental setup different from the one presented here (see e.g. Ref. [10]). In our demonstration, we have left the spectral phases of the harmonics unchanged and taken their values from measurements performed under nearly identical conditions [22] (argon as generation medium, pulse intensity $1.2 \cdot 10^{14}$ W/cm^2).

The result of the calculations is shown in Fig. 4: panel 4(B) shows the attosecond XUV waveform corresponding to the unshaped HH spectrum (shown in Fig. 3(g))and panel 4(A) the attosecond waveform corresponding to the shaped spectrum in which H11 has been maximally attenuated (as in Fig. 3(a)). The amplitude shaping demonstrated in the present work has a dramatic effect on the attosecond waveform, which will be instrumental in controlling non-linear processes in the XUV and the realization of coherent control experiments using XUV radiation.

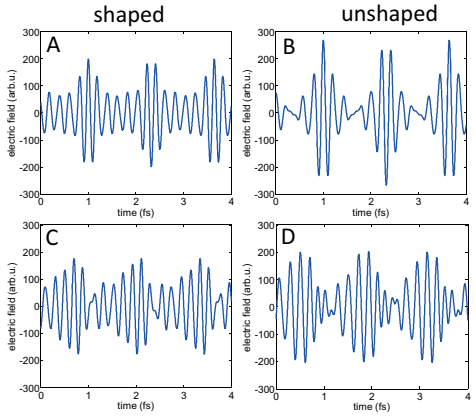

Fig. 4. Simulation of the temporal structure of the XUV electric fields composed of the observed harmonics H11-H19 with the measured intensities, after (A and C) and before (B and D) the pulse shaper. The upper row shows the XUV waveforms obtained by assuming a flat spectral phase across the observed harmonic orders, whereas the lower row shows the XUV waveforms obtained when using the spectral phase measured under nearly identical conditions [22].

We now study the influence of the attochirp on the calculated waveforms (Fig. 4(c) and 4(d)). Just as in the case of a flat spectral phase, we find that our amplitude shaping has a pronounced effect on the temporal structure of the attosecond waveform.

Although demonstrated with discrete harmonics, our XUV waveform shaper will also enable perfect amplitude control of continuous spectra associated with isolated attosecond pulses,

#174409 - $15.00 USD Received 16 Aug 2012; revised 18 Sep 2012; accepted 18 Sep 2012; published 1 Nov 2012

bringing attosecond pulse shaping within reach. Moreover, the MEMS device used in our experiment is able to provide simultaneously tilt and stroke motion [19] (see supplementary movie Media 4) such that phase shaping can be added to amplitude shaping. Using our device, one could simultaneously compensate the attochirp and imprint an arbitrary phase mask onto the isolated attosecond pulse, opening a vast field of applications in attoscience.

Acknowledgments

We thank S. Vlajkovic for his contribution to the experiment. We acknowledge W. Noell, F. Jutzi and N. De Rooij from IMT-EPFL and J. Extermann and S. Weber from Univ. Geneva, for their seminal contribution in the development of the MEMS device. We also acknowledge the Swiss NSF through the NCCR Quantum Photonics in this respect, and the NCCR MUST for the present work. P. M. Kraus and H.J. Wörner gratefully acknowledge funding from the Swiss NSF (PP00P2_128274).

#174409 - $15.00 USD Received 16 Aug 2012; revised 18 Sep 2012; accepted 18 Sep 2012; published 1 Nov 2012